Magnetic confinement of a high-density cylindrical plasma

Eduardo Ahedo[a)]
E. T. S. Ingenieros Aeronáuticos, Universidad Politécnica de Madrid, Madrid 28040, Spain

(Received 28 February 2011; accepted 13 September 2011; published online 18 October 2011)

The stationary structure of a weakly collisional plasma column, confined by an axial magnetic field and a cylindrical vessel, is studied for the high-density case, when the diamagnetic azimuthal current is large enough to demagnetize partially the plasma. The plasma response is characterized mainly by two dimensionless parameters: the ratios of the electron gyroradius and the electron skin-depth to the plasma radius, and each of them measures the independent influence of the applied magnetic field and the plasma density on the plasma response. The strong magnetic confinement regime, characterized by very small wall losses, is limited to the small gyroradius and large skin-depth ranges. In the high-density case, when the electron skin-depth is smaller than the electron gyroradius, the skin-depth turns out to be the magnetic screening length, so that the bulk of the plasma behaves as unmagnetized. [doi:10.1063/1.3646923]

I. INTRODUCTION

A plasma contained in a cylindrical vessel and affected by an axial magnetic field is a classical confinement configuration. The first detailed analysis of the problem dates back to the radial diffusive model of Tonks,[1] who showed the formation and central role of the azimuthal plasma current. Later, Forrest and Franklin[2] and Ewald *et al*.[3] included ion inertia effects for a weakly collisional plasma. In the last years, the problem has been revisited by several authors. Sternberg *et al*.[4] have highlighted that, for a magnetized plasma, the electron force balance involves the expanding pressure gradient and the confining magnetic force caused by the plasma current, so that the Boltzmann relation does not apply to electrons. Our contribution[5] has been to carry out a detailed asymptotic and parametric analysis of the problem, which has shown that: (1) the inertial layer linking the bulk diffusive region to the Debye sheath is initiated by electron-inertia effects that tend to limit the growth of the electron azimuthal current; (2) ion-inertia effects are limited to a subregion within that layer; and (3) the change from the magnetic to the electric force as main confining force on electrons takes place *within* the ion-inertia sublayer, when the ion Mach number is about 0.7. In addition, we showed the existence of a second distinguished magnetized regime when electron collisionality is very small, and we provided simple scaling laws for particle and energy fluxes to the wall (which measure the magnetic confinement level of the plasma column).

In our analysis, the main magnetized regime is characterized by the distinguished limits

$$\lambda_{d0} \ll \ell_{e0} \ll R \sim c_s/\nu_e, \tag{1}$$

$$\beta_0 \ll 1, \tag{2}$$

where R is the radius of the plasma column, $\lambda_{d0} = \sqrt{\varepsilon_0 T_e/e^2 n_0}$ is the Debye length, with T_e the electron temperature and n_0 the plasma density at the axis; $\ell_{e0} = \sqrt{T_e m_e}/eB_0$ is the electron gyroradius, with B_0 the externally applied magnetic field; $c_s = \sqrt{T_e/m_i}$ is the plasma sound speed and ν_e is the electron collision frequency; and $\beta_0 = \mu_0 n_0 T_e/B_0^2$ is *half the* ratio between thermal and magnetic pressures. Conditions (1)-(2) assure that the plasma is magnetized, weakly collisional, and quasineutral except in the thin Debye sheath adjacent to the wall.

It is well known—for instance from the MHD equilibrium of a θ-pinch[6]—that the azimuthal plasma current is diamagnetic and induces a magnetic field that opposes the applied one. The induced field is negligible in the low-density or zero-beta limit, Eq. (2), but otherwise it makes the total magnetic field to have a minimum at the center of the plasma column.[6,7] Nonzero-β_0 effects are of interest to high-density plasmas. For instance, helicon thrusters, in order to be competitive, require[8–12] a moderate magnetic field [$\sim$0.01–0.05 T], a high plasma temperature ($\sim$20–30 eV), and a relatively high density ($\sim 10^{19}\mathrm{m}^{-3}$), so that values of β_0 about 0.5 can be reached.

This paper attempts to characterize the nonzero-beta regime of a cylindrical plasma satisfying conditions (1). Specific goals of the study are, first, to determine the changes caused by β_0 in the radial plasma structure and in the magnetic confinement of the plasma column, and, second, the different parametric regimes of the plasma response. Interestingly, the collisionless electron skin-depth, generally related to time-dependent problems, such as inductive plasma discharges[13,14] or hydromagnetic solitary waves,[15] will turn out to be a characteristic length of both the plasma spatial profile and the confinement regime. Finally, the competition between the ambipolar electric field and the total magnetic field in confining the plasma column[4,5,7] is commented.

II. MODEL FORMULATION

In order to tackle with nonzero-beta effects, the Ampere's law must be added to the zero-beta, cylindrical

a)Electronic mail: eduardo.ahedo@upm.es.

model of Ref. 5. Neglecting terms that we showed there to be small, the relevant set of equations for the quasineutral plasma column are

$$\frac{1}{r}\frac{d}{dr}(rn_e u_r) = n_e \nu_w, \tag{3}$$

$$0 = -\frac{1}{n_e}\frac{d}{dr}(T_e n_e) + e\frac{d\phi}{dr} - eu_{\theta e}B + m_e\frac{u_{\theta e}^2}{r}, \tag{4}$$

$$m_i u_r\frac{du_r}{dr} = -e\frac{d\phi}{dr} - m_i\nu_i u_r, \tag{5}$$

$$m_e u_r\frac{du_{\theta e}}{dr} = eu_r B - \nu_e m_e u_{\theta e} - m_e\frac{u_{\theta e}u_r}{r}, \tag{6}$$

$$\frac{dB}{dr} = \mu_0 e n_e u_{\theta e}, \tag{7}$$

where n_e is the density of the quasineutral plasma; $u_r = u_{re} = u_{ri}$ is the radial velocity of both ions and electrons, consistent with a one-dimensional model and a dielectric wall; $u_{\theta e}$ is the electron azimuthal velocity; B is the local magnetic field; φ is the ambipolar electric potential; $\nu_i = \nu_{ion} + \nu_{in}$ is the ion total collision frequency, with contributions of the ionization frequency and the ion-neutral collision frequency; $\nu_e = \nu_{ion} + \nu_{en} + \nu_{ei}$ is the electron total collision frequency, with contributions of ν_{ion} and the electron-neutral and electron-ion collision frequencies; and ν_w is the frequency for plasma losses at the wall. This loss frequency is indeed an eigenvalue of the problem and must satisfy the plasma balance condition,[16] which states that, in the stationary response, plasma losses at the wall are equal to the volumetric plasma production (i.e., $\propto \nu_{ion}$) plus any axial differential transport [$\propto (\nu_w - \nu_{ion})$ in this one-dimensional model]. Equations (3)–(7) do not include the ion azimuthal velocity, which was shown to be negligible in practical cases,[5] $u_{\theta i}/u_{\theta e} \sim m_e\nu_i/(m_i\nu_e)$. Also the ion pressure has been neglected and hereafter we will take T_e, ν_e, and ν_i as known constants. These assumptions simplify the discussion without affecting the core and aims of the present study.

Manipulating Eqs. (3)–(5) allows us to solve for the derivatives of u_r and n_e,

$$m_i\left(\frac{c_s^2}{u_r} - u_r\right)\frac{du_r}{dr} = eu_{\theta e}B + m_i\left(\nu_i u_r + \nu_w\frac{c_s^2}{u_r}\right) - \frac{m_i c_s^2 + m_e u_{\theta e}^2}{r}, \tag{8}$$

$$u_r\frac{dn_e}{dr} = n_e\left(\nu_w - \frac{u_r}{r} - \frac{du_r}{dr}\right), \tag{9}$$

and then to solve Eq. (5) for the derivative of ϕ. Now, the set of Eqs. (5)–(9) constitute a standard first-order system of differential equations, which presents singularities at $r = 0$, $u_r = 0$, and $u_r = c_s$. The two first ones take place at the plasma axis and they are avoided by just eliminating unbounded modes there [see boundary condition (12) in Ref. 5]. The third one is the classical sonic singularity and matches with the Bohm condition at the edge S of the Debye sheath. In the asymptotic analysis consistent with Eq. (1), the Debye sheath is a discontinuity between the quasineutral plasma and the wall W, so that we can take $r_S = R$ in the quasineutral scale. Therefore, the six boundary conditions for the five plasma equations *and* the eigenvalue ν_w are $n_e = n_0$, $u_r = 0$, $u_{\theta e} = 0$, and $\phi = 0$ at the plasma axis ($r = 0$), and $u_r = c_s$ and $B = B_0$ at the sheath edge S (i.e., $r \simeq R$).

Equations (5)–(9) are non-dimensionalized as in Ref. 5, and this process identifies the set of free parameters that determine the plasma response. Here, Eq. (7) introduces β_0 as a new free parameter and the dimensionless plasma balance equation takes the functional form

$$\frac{\nu_w R}{c_s} = \hat{\nu}_w\left(\frac{\ell_{e0}}{R}, \frac{\bar{\lambda}_e}{R}, \frac{R\nu_i}{c_s}, \beta_0\right), \tag{10}$$

where $\bar{\lambda}_e = c_s/\nu_e$ is a *reduced* (by the square of the electron-to-ion-mass ratio) collisional mean-free path for electrons. It was shown in Ref. 5 that the ion-collision parameter $R\nu_i/c_s$ has a minor role in the response and the scaling laws for the magnetized regime, so discussions here will assume implicitly that $R\nu_i/c_s \ll 1$.

The electron skin-depth $d_{e0} = \sqrt{m_e/(e^2\mu_0 n_0)}$ satisfies $\beta_0 = \ell_{e0}^2/d_{e0}^2$. Therefore, d_{e0}/R can be used as free parameter instead of β_0. Indeed, since

$$\ell_{e0} \propto B_0^{-1}, \qquad d_{e0} \propto n_0^{-1/2}, \tag{11}$$

the pair of parameters (ℓ_{e0}/R, d_{e0}/R) is clearly more appropriate than the pair (ℓ_{e0}/R, β_0) for studying the independent effects of the applied magnetic field and the density on the plasma response. Since n_0 is present only in β_0 (or in d_{e0}/R), the nonzero-beta case brings with it all the influence of the plasma density on the dimensionless response of the plasma column. Zimmerman *et al.*,[7] who include Ampere's law and present particular solutions with the induced magnetic field, miss somehow β_0 among their model parameters (notice that their β_0 and χ are indeed comparable to ours R/ℓ_{e0} and $\bar{\lambda}_e/\ell_{e0}$, respectively, and none of them include the product $\mu_0 n_0$, present in β_0).

III. PLASMA RESPONSE

A. Zero-beta limit

We briefly summarize here results of Ref. 5 that are of interest for the nonzero-beta study. For $\beta_0 \to 0$, Eq. (7) yields $B(r) = B_0$. Then, the asymptotically exact solution of the diffusive bulk region is

$$\frac{n_e}{n_0} = J_0\left(a_0\frac{r}{R}\right), \qquad \frac{n_e u_{\theta e}}{n_0 c_e} = \frac{\ell_{e0}}{R}a_0 J_1\left(a_0\frac{r}{R}\right), \qquad \frac{u_r}{c_s} = \frac{u_{\theta e}}{c_e}\frac{\ell_{e0}}{\bar{\lambda}_e}, \tag{12}$$

with J_0 and J_1 Bessel functions and $a_0 \simeq 2.405$ the first zero of J_0. Notice that u_r with c_s and $u_{\theta e}$ are normalized with c_s and $c_e = \sqrt{T_e/m_e}$ respectively. The transition to the inertial layer takes place when $u_{\theta e} = O(c_e)$. Within this layer, of thickness $O(\ell_{e0})$ roughly, electron inertia hinders further increments of $u_{\theta e}$. Then, in a shorter sublayer [see Eq. (31) of Ref. 5], ion inertia brings u_r/c_s from $O(\ell_{e0}/\bar{\lambda}_e)$ to 1, and the ambipolar electric force surpass the magnetic force at $u_r/c_s \simeq 2^{-1/2}$.

The plasma flux to the wall (also constant across the inertial and Debye layers) is $n_{eS}c_s$ with

$$\frac{n_{eS}}{n_0} \simeq 1.25\frac{\ell_{e0}^2}{R\bar{\lambda}_e}. \tag{13}$$

This illustrates the excellent confinement provided by the applied magnetic field; for instance, experimental measurements by Tysk *et al.*[17] yield $n_{eS}/n_0 \sim 1\%$. Equation (13) has to be compared with

$$\frac{n_{eS}}{n_0} = \mathrm{e}^{-1/2} \simeq 0.61, \tag{14}$$

for an unmagnetized, weakly collisional plasma, which is confined only electrostatically, by the ambipolar electric field set up by the presence of the wall.

B. Nonzero beta regimes

For $\beta_0 \ll 1$, the small induced magnetic field can be obtained by solving Eq. (7) with the zero-beta solution (12) on the right-hand side,

$$\frac{dB}{dr} \simeq \beta_0 B_0 \frac{a_0}{R} J_1\left(\frac{a_0 r}{R}\right). \tag{15}$$

Straightforward integration yields

$$1 - B(r)/B_0 \simeq \beta_0\, J_0(a_0 r/R), \qquad (\beta_0 \ll 1), \tag{16}$$

and the minimum value of the magnetic field is $B(0) \simeq (1-\beta_0)B_0$, at the plasma column axis.

When β_0 is no longer small, Eq. (7) must be solved together with the rest of plasma equations but Eq. (16) already suggests that the central part of the plasma column is demagnetized. Let us take the case of a plasma with $\ell_{e0}/R \ll 1$ and analyze the plasma response as its density at the axis is increased, that is as d_{e0}/R is decreased or β_0 is increased. Figure 1 plots the radial profiles of plasma magnitudes for $\ell_{e0}/R = 0.1$ and different values of β_0 in the range between 0 and 2.5, that is $\infty > d_{e0}/R > 0.032$. Figure 1(a) shows how the total magnetic field decreases as β_0 increases. The central plasma region becomes totally demagnetized for $\beta_0 \sim 0.5$, and magnetization is limited to a thin layer near the wall when $\beta_0 > 1$. Figure 1(b) depicts the density profile, illustrating how magnetic confinement deteriorates as β_0 increases. Figure 1(c) plots u_r: the gentler profiles as β_0 increases are due to a larger electrostatic field in the central region. As the dashed lines of Figs. 1(b) and 1(c) corroborate, the behavior of a plasma with $\ell_{e0}/R \ll 1$ and β_0 large approaches that of the unmagnetized case $\ell_{e0}/R = \infty$, except in a thin demagnetization layer. The profiles of $u_{\theta e}$ in Fig. 1(d) are the consequence of two facts: (1) $u_{\theta e}$ provides the resistive force that opposes the azimuthal magnetic force, Eq. (6), and (2) the larger n_0 is, the lower is the value of $u_{\theta e}$ required to generate the current required to screen the applied magnetic field, Eq. (7). Figure 1(e) shows that the profiles of $j_{\theta e} = -en_e u_{\theta e}$ change significantly with β_0, and they reflect the fact that $j_{\theta e}$ is the product of variables with different trends as β_0 is varied.

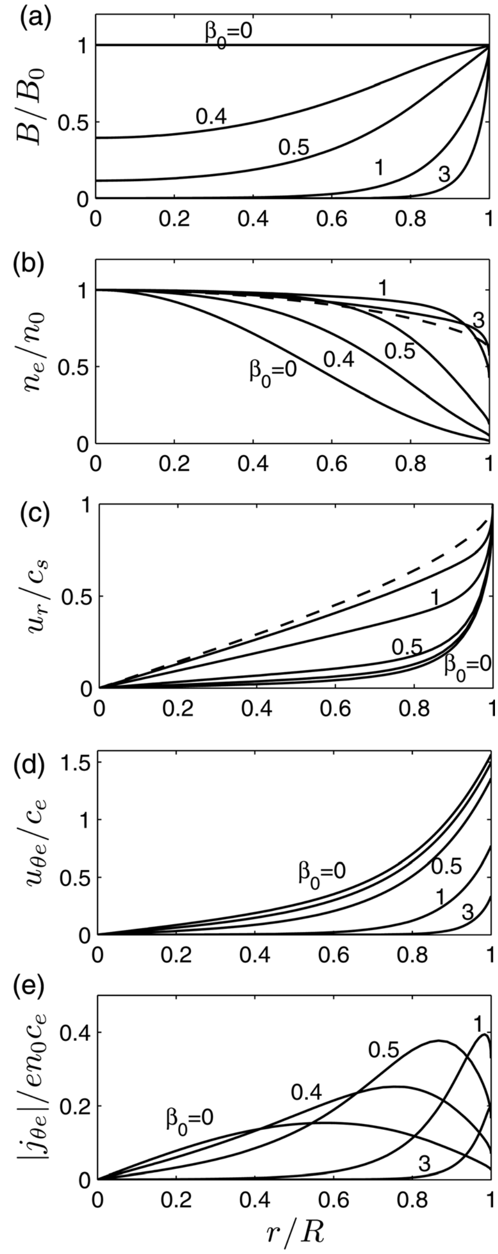

FIG. 1. Plasma profiles for $\ell_{e0}/R = 0.1$ and $\beta_0 = 0$, 0.4, 0.5, 1, and 3 (solid lines), corresponding to $d_{e0}/R \simeq \infty$, 0.16, 0.14, 0.10, and 0.058. Dashed lines correspond to the unmagnetized case $\ell_{e0}/R = \infty$. Other parameters for all curves are $\bar{\lambda}_e/R = 1$ and $R\nu_i/c_s \to 0$.

Therefore, for $\beta \geq O(1)$, the magnetized plasma and $j_{\theta e}$ are limited to a thin quasineutral layer adjacent to the Debye sheath. The characteristic thickness of that layer is the electron skin-depth, d_{e0}, as the plots suggest and we confirm next with the plasma equations. For $\ell_{e0}/R \ll 1$ and $\beta_0 \geq O(1)$, the dominant form, *near the sheath edge* of Eq. (6) is $m_e du_{\theta e}/dr \simeq eB$. This yields $u_{\theta eS} \sim (eB_0/m_e)\Delta r$, with Δr the layer thickness. Then, Eq. (7) yields $\Delta r \sim d_{e0}$ and

$$u_{\theta eS} \sim c_e \beta_0^{-1/2}. \tag{17}$$

A characterization of the combined effects of ℓ_{e0}/R and d_{e0}/R on the plasma response is provided by the parametric curves of Figs. 2 and 3. The normalized (or dimensionless)

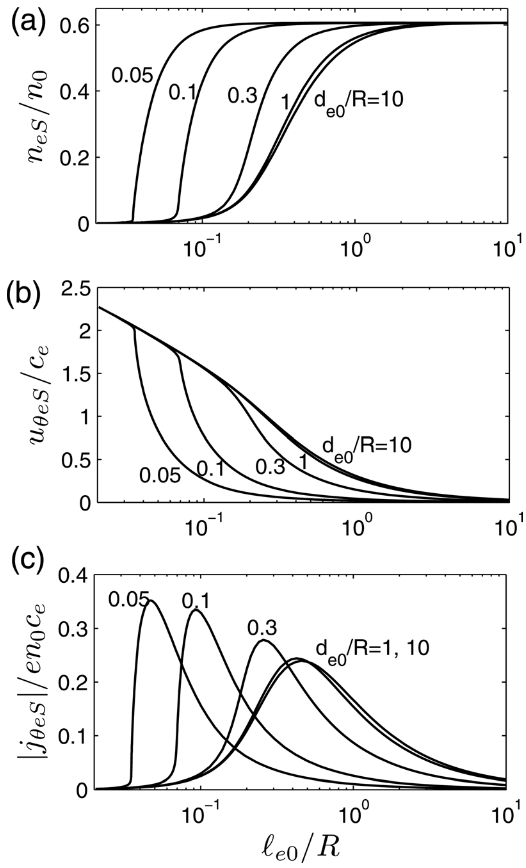

FIG. 2. Plasma response versus ℓ_{e0}/R for $d_{e0}/R = 10$, 1, 0.3, 0.1, and 0.05; other parameters are $\bar{\lambda}_e/R = 1$ and $R\nu_i/c_s \to 0$. (a) Normalized plasma density at the sheath edge, which coincides with the normalized plasma flux to the wall. (b)–(c) Normalized azimuthal velocity and current of electrons at the edge of and within the Debye sheath.

plasma flux to the wall is plotted in Fig. 2(a). Figures 2(b) and 2(c) plot the electron azimuthal velocity and current at the sheath edge, which are also a measure of the plasma magnetization level. There are three regions in the curves of Fig. 2(a): (1) for ℓ_{e0}/R small enough, the plasma is magnetically confined with $n_{eS}/n_0 \ll 1$; (2) for ℓ_{e0}/R large, the plasma is unmagnetized and confined only electrostatically, with $n_{eS}/n_0 \simeq 0.6$; (3) for intermediate values of ℓ_{e0}/R, the transition between those distinguished regimes takes place. As d_{e0}/R decreases from about 1, the range of ℓ_{e0}/R corresponding to magnetic confinement is reduced.

Figure 3(a) plots the normalized plasma flux to the wall versus $\ell_{e0}/d_{e0} \equiv \beta_0^{1/2}$, in the range $d_{e0}/R < 1$ of interest here. This figure shows that the magnetic confinement regime ends quite abruptly at $\ell_{e0}/d_{e0} \simeq 0.7$, i.e., at $\beta_0 \simeq 0.5$. Figure 3(b) shows that this limit corresponds approximately to the case of the total magnetic field at the plasma axis becoming negligible. From $\beta_0 \simeq 0.5$, up there is a transition regime that ends around $\ell_{e0}/d_{e0} \approx 2$, i.e., at $\beta_0 \approx 4$ when the plasma flux to the wall corresponds again to electrostatic confinement. For $\beta_0 > 4$, the plasma column is magnetized only in a thin layer around the wall, of thickness $\sim d_{e0}$, with no effect on plasma confinement. The location of magnetic and electrostatic confinement regimes in the parametric plane $(\ell_{e0}/R, d_{e0}/R)$ is illustrated in Fig. 4, where constant flux-to-the-wall curves are plotted. The two selected curves,

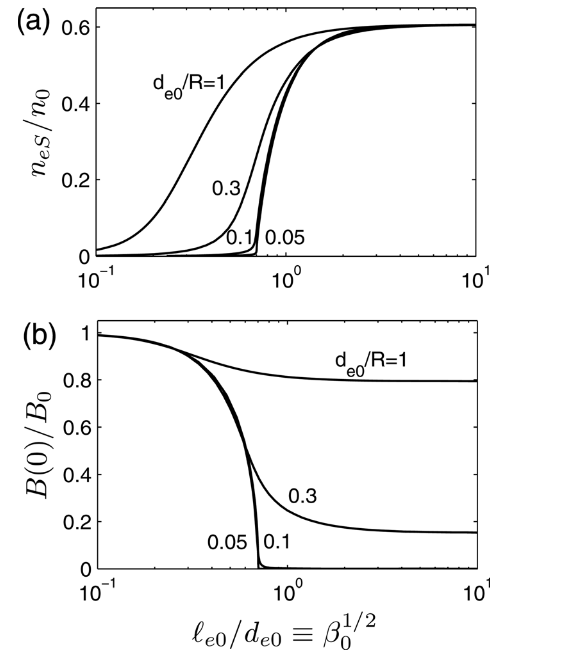

FIG. 3. Plasma response versus $\ell_{e0}/d_{e0} \equiv \beta_0^{1/2}$ for $d_{e0}/R = 1$, 0.3, 0.1, and 0.05; other parameters are $\bar{\lambda}_e/R = 1$ and $R\nu_i/c_s \to 0$. (a) Normalized plasma density at the sheath edge, which coincides with the normalized plasma flux to the wall. (b) Total magnetic field at the plasma axis relative to the applied magnetic field.

$n_{eS}/n_0 = 0.05$ and 0.5, could serve as approximate boundaries of the magnetic, electrostatic, and intermediate confinement regimes. Finally, notice that the above analysis has been centered in the weakly collisional limit, when the Hall parameter, $\bar{\lambda}_e/\ell_{e0}$, is very large. Collisional effects, which tend to reduce magnetic confinement, were already discussed in Ref. 5.

C. Force balance

The sum of Eqs. (4) and (5), together with the Ampere's law (7) yields the radial momentum equation of the plasma in the form

$$m_i n_e u_r \frac{du_r}{dr} = -\frac{d}{dr}\left(T_e n_e + \frac{B^2}{2\mu_0}\right) - m_i n_e \nu_i u_r + m_e n_e \frac{u_{\theta e}^2}{r}, \quad (18)$$

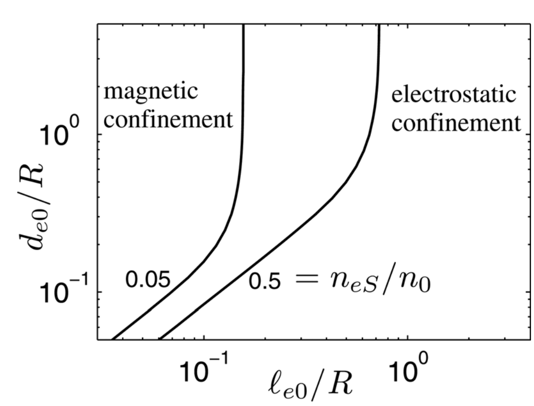

FIG. 4. Curves of constant plasma flux to the wall: $n_{eS}/n_0 = 0.5$ and 0.05, in the parametric plane $(\ell_{e0}/R, d_{e0}/R)$. Other parameters are $\bar{\lambda}_e/R = 1$ and $R\nu_i/c_s \to 0$.

where the magnetic pressure appears explicitly as complementing the thermal pressure. For $\ell_{e0}/R \ll 1$ and $0 < \beta_0 \ll 1$, the plasma response in the bulk region corresponds to the known θ-pinch or constant-pressure equilibrium[6]

$$T_e n_e + B^2/(2\mu_0) = \text{const.} \tag{19}$$

Then, in the inertial layer, ion convection becomes significant, and, finally, the magnetic force is negligible in the Debye sheath. However, for $\beta_0 = O(1)$, when induced magnetic effects are large, the above constant pressure law holds nowhere because of the ion inertia term is relevant already in the bulk region. Apart from showing the similarity with the basic θ-pinch equilibrium, expressing the magnetic force term, $j_{\theta e}B$, as the gradient of the magnetic pressure does not present any advantage when solving the present problem. For β_0 small, most of the contribution to the magnetic pressure comes from the applied field, which is constant and has a zero contribution to the pressure gradient. Indeed, the magnetic pressure gradient term of Eq. (18), which is proportional to $(dB/dr)/\beta_0$, appears as a mathematically indeterminate expression of the form $0/0$ in the asymptotic limit $\beta_0 \to 0$; therefore, the equivalent form $j_{\theta e}B$, which does not present that mathematical issue, is preferable.

The electron force balance, given by Eq. (4), can be expressed as

$$f_p + f_c = f_e + f_m \equiv f, \tag{20}$$

with $f_p = -T_e\, d\ln n_e/dr$, $f_c = m_e u_{\theta e}^2/r$, $f_e = -ed\varphi/dr$, and $f_m = eu_{\theta e}B$. Each term in Eq. (20) is positive and represents a force contribution *on an "average" electron*. The pressure gradient, f_p, and the centrifugal force, f_c, are expansion forces, grouped in the left-hand side of Eq. (20); the electric force, f_e, and the magnetic force, f_m, confine the electrons. Notice from Eq. (5) that, when ion resistivity and ion pressure are negligible, f_e is the only force on an "average" ion, and accelerates it towards the wall.

Figure 5 plots $f_c/f \equiv 1 - f_p/f$ and $f_m/f = 1 - f_e/f$ at different spatial locations and different values of β_0, for a plasma with $\ell_{e0}/R = 0.10$. This representation facilitates a quick assessment of the relevance of each of the four forces to the balance of Eq. (20). First, the thermal pressure gradient is by far the main contribution to the electron expansion, i.e., $f \simeq f_p$; the centrifugal contribution f_c/f is relevant only in the collisionless (i.e., $R \ll \bar{\lambda}_e$), intermediate-magnetization regime of Ref. 5. Then, the solid lines of Fig. 5 illustrate on the competition between electric and magnetic forces in confining electrons, the dominant force changing both with the *radial* location and the *parametric* point in the plane $(\ell_{e0}/R, d_{e0}/R)$. Starting with the parametric influence, the magnetic force is stronger, on the average, the lower are ℓ_{e0}/R and β_0, and it is marginal *at any* r for β_0 large, even when $\ell_{e0}/R \ll 1$. With respect to the dominant force at different radial locations, the electric force dominates *always* in the region $u_r/c_s \gtrsim 0.7$ independently of ℓ_{e0}/R and β_0. In addition, for $\ell_{e0}/R \ll 1$, the electric force becomes dominant in the central region for moderate values of β_0. At the sheath edge limit $u_r/c_s \to 1$, one has $f_m/f \to 0$, that is $f_m/f_e \to 0$. The magnetic force at the sheath edge is $f_{mS} = eu_{\theta eS}B_0$, with $u_{\theta eS}$ plotted in Fig. 2(b). Thus, the vanishing of the magnetic-to-electric force ratio is due to the known singular behavior of the ambipolar electric field there, i.e., $f_{eS} \to \infty$.

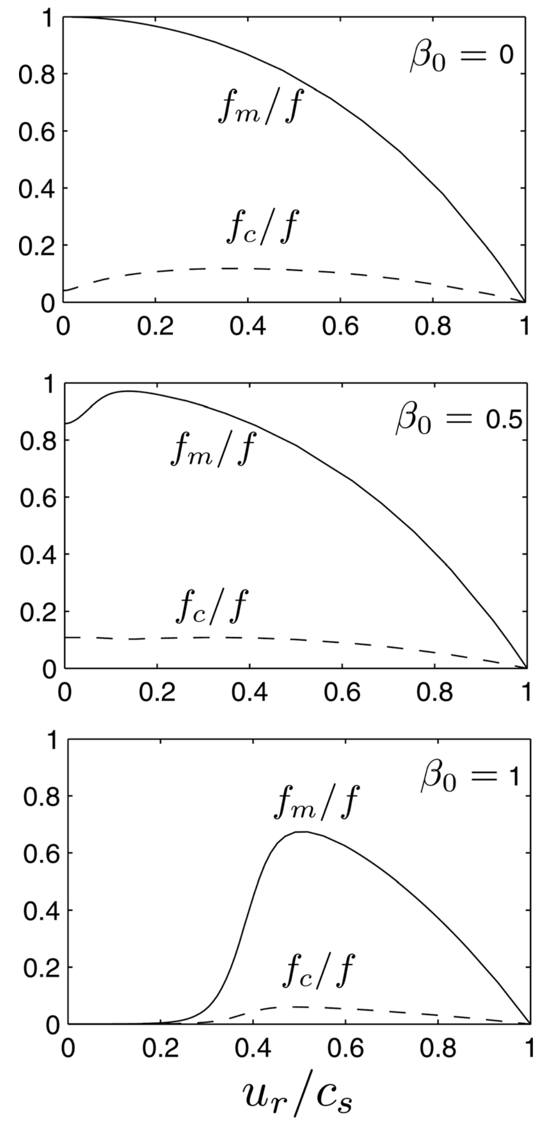

FIG. 5. Relative strength of each force contribution to the electron force balance, Eq. (20), for three values of β_0. Other parameters are $\ell_{e0}/R = 0.10$, $\bar{\lambda}_e/R = 1$, and $R\nu_i/c_s \to 0$. Notice that $f_p/f = 1 - f_c/f$, $f_e/f = 1 - f_m/f$, and u_r is used as abscissa instead of r.

IV. CONCLUSIONS

The strong diamagnetic current and the induced magnetic field that arise in a magnetized cylindrical plasma when the thermal-to-magnetic pressure ratio is not small cause important changes in the plasma behavior. For a zero-Debye-length and weakly collisional plasma, the problem is characterized by two dimensionless parameters, ℓ_{e0}/R and either d_{e0}/R or β_0. These parameters depend on the applied magnetic field and the plasma density at the axis. The strong magnetic confinement regime, characterized in a previous work for $\beta_0 = 0$, is found here to be limited to $\ell_{e0}/R \ll 1$ and $\beta_0 < 0.5$. For $\beta_0 > 0.5$, the central region of the column is demagnetized, which allows the development of the electric force and ion acceleration there, and increases the plasma flux to the wall. For $\beta_0 > 3-4$ roughly, the plasma is unmagnetized except in a thin layer near the wall, but the confinement is electrostatic. Interestingly, the electron skin-depth is the *magnetic screening length* of this stationary, large-beta, plasma column.

To summarize, a magnetically confined plasma, crucial to have small recombination and energy losses at the vessel walls, requires the electron gyroradius, based on the applied magnetic field, be smaller than three typical lengths: the plasma radius, a (reduced) collisional mean free path for electrons, and the electron skin depth. The two last lengths depend on plasma density and temperature.

ACKNOWLEDGMENTS

This work has been sponsored by the Air Force Office of Scientific Research, Air Force Material Command, USAF, under Grant number FA8655-10-1-3085. The U.S Government is authorized to reproduce and distribute reprints for Governmental purpose notwithstanding any copyright notation thereon. Additional support came from the Gobierno de España (Project No. AYA2010-16699). The author thanks Dr. Mitat Birkan for his support.

[1] L. Tonks, Phys. Rev. **56**, 360 (1939).
[2] J. Forrest and R. Franklin, Br. J. Appl. Phys. **17**, 1061 (1966).
[3] H. Ewald, F. Crawford, and S. Self, J. Appl. Phys. **38**, 2753 (1967).
[4] N. Sternberg, V. Godyak, and D. Hoffman, Phys. Plasmas **13**, 063511 (2006).
[5] E. Ahedo, Phys. Plasmas **16**, 113503 (2009).
[6] J. Freidberg, *Plasma Physics and Fusion Energy* (Cambridge University Press, Cambridge, 2007).
[7] T. Zimmermann, M. Coppins, and J. Allen, Phys. Plasmas **17**, 022301 (2010).
[8] R. Winglee, T. Ziemba, L. Giersch, J. Prager, J. Carscadden, and B. R. Roberson, Phys. Plasmas **14**, 063501 (2007).
[9] O. Batishchev, IEEE Trans. Plasma Sci. **37**, 1563 (2009).
[10] D. Pavarin, F. Ferri, M. Manente, D. Curreli, Y. Guclu, D. Melazzi, D. Rondini, S. Suman, J. Carlsson, C. Bramanti, E. Ahedo, V. Lancellotti, K. Katsonis, and G. Markelov, Design of 50 W Helicon Plasma Thruster," in *31th International Electric Propulsion Conference, Ann Arbor, Michigan, USA, IEPC 2009-205* (Electric Rocket Propulsion Society, Fairview Park, OH, 2009).
[11] E. Ahedo, "Cylindrical model of a helicon-generated plasma," in *31th International Electric Propulsion Conference, Ann Arbor, Michigan, USA, IEPC 2009-193* (Electric Rocket Propulsion Society, Fairview Park, OH, 2009).
[12] E. Ahedo and M. Merino, Phys. Plasmas **17**, 073501 (2010).
[13] L. Spitzer, *Physics of Fully Ionized Gases* (Wiley, New York, 1962).
[14] M. Lieberman and A. Lichtenberg, *Principles of Plasma Discharges and Materials Processing* (Wiley, Hoboken, NJ, 2005).
[15] J. Adlam and J. Allen, Philos. Mag. **3**, 448 (1958).
[16] L. Tonks and I. Langmuir, Phys. Rev. **34**, 876 (1929).
[17] S. Tysk, C. Denning, J. Scharer, and K. Akhtar, Phys. Plasmas **11**, 878 (2004).